Vertiport Throughput Capacity under Constraints caused by Vehicle Design, Regulations and Operations

Lukas Preis[1] and Manuel Hack Vazquez[1]

[1] Bauhaus Luftfahrt e.V.
Lukas.Preis@bauhaus-luftfahrt.net

Abstract

Urban Air Mobility has the potential to substantially reduce travel times in some cases of urban-related transportation. Travel time savings strongly depend on fast processing at vertiports, which presents a key challenge considering demand levels vertiports would experience when becoming an established mode of transport. This paper sheds light on the passenger throughput capacity vertiport airfields can manage and how the operations are sensitive to changes. Three studies are presented in this paper: a baseline study, a vehicle study and a study of safety margins. Some of the key insights are: (1) For the vehicle *VoloCity* 0.015 passengers can be served in one hour per square meter airfield area. (2) Comparing various prominent vehicles it was found that the *CityAirbus* performs best. (3) The biggest potential of increasing throughput by reducing safety margins lies in shrinking the aircraft separation minima during approach and departure operations. The insights presented in this paper might be useful for researches, vehicle developers and regulatory agencies alike.

1 Introduction and literature review

Urban Air Mobility (UAM) is an emerging transportation concept that has the potential to enrich the existing transport system through a new mode with the particular advantage of reducing travel times. The introduction of UAM faces severe hurdles [1], among which infrastructure presents a key issue [2–4]. Next to the aircraft-specific issues around Electric Vertical Take-Off and Landing Vehicles (eVTOLs), there are various hurdles to overcome, such as air traffic management [5–13], noise [14–17] or safety and certification [18–20]. Many of these issues are already being addressed [21–24] while the question of ground infrastructure finds secondary attention. In particular the locating and sizing of vertiports has recently been identified as a significant research gap [25].

In a previous publication a Mixed-Integer Programming (MIP) approach for sizing and designing vertiports has been presented by Preis [26] with the aim of closing this research gap. The present work applies this MIP approach to analyze vertiport sensitivities. Further publications that should find mention here are Vascik's ground-breaking analysis of vertiport capacities, which served as inspiration for this work [27]. Another important work is by Zelinski, who looked at vertiport design in a holistic sense, considering among other things weather impact and vertiport topologies [28]. A patent for dynamic vertiport configurations was published by Alexander [29] and efforts to craft an ISO standard for vertiports is under way [30].

2 Method and baseline scenario

2.1 Vertiport sizing method

In this section the Vertiport Sizing Method (VSM) published by Preis [26] will be re-iterated briefly and applied to a baseline vertiport scenario, which will serve as reference for the following sensitivity analysis. The VSM uses MIP in a branch-and-bound fashion with a utility function of maximizing hourly vehicle and passenger throughput. Vehicle throughput is defined as (1) approach of the vehicle from the airspace and landing on a pad, (2) taxiing to a gate, (3) turnaround at the gate including passenger boarding and de-boarding, (4) taxiing back to a pad, and (5) take-off and departure into the airspace (see figure 1). Based on the size and shape of a given surface area the optimal vertiport

airfield design is estimated, including the number of pads and gates, a suggestion for the topology and the maximum possible hourly throughput. There are four topologies, which are compared for each scenario: single-pad, satellite, linear and pier (see figure 2). Each topology has a range of sub-layouts, which are presented in detail by Hack Vazquez [31]. Assumptions for the dimensions of pads, gates and taxi-ways, including their safety zones are derived from the "Heliport Design Guidelines" published by the *Advisory Circle 150/5390-2C* of the FAA [32].

Figure 1: Definition of vehicle throughput

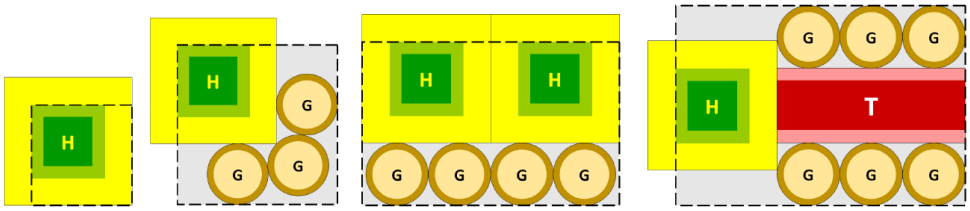

Figure 2: Vertiport topologies considered in the vertiport sizing method: single, satellite, linear, pier

2.2 Definition baseline scenario

The operational parameters required by the VSM are shown in table 1 and the values are chosen according to previous vertiport parameter specification [33] and aggregation [34]. The parameter values were determined through extensive literature review and an expert interview series (n=17), which included refining the model itself. Approach & landing and take-off & departure of vehicles are each aggregated into one parameter and correspond to the time a pad is occupied with the respective operation. As reference vehicle the *VoloCity* from Volocopter was chosen (see figure 3) with two seats and a tip-to-tip span and maximum dimension of both 11.3 m [35]. The taxi-mode is hovering close to the surface with engines being shut-off after touch-down at the gate. For simultaneous operations of pads the distance between their two Final Approach and Take-Off Area (FATO) must be at least 200 ft according to the "Heliport Design Guidelines" by FAA [32]. All parameter values are listed in table 1.

Two variations of the baseline scenario are presented: (1) a vertistop, with no fixed turnaround time and vehicle operations assumed to be done in a touch-and-go fashion. (2) A vertihub, with a fixed turnaround time of 20 minutes, which might entail charging, battery swapping or minor MRO activities. It is assumed that vehicle-related turnaround and passenger boarding can happen simultaneously; the longer time of both determines to overall turnaround time. For more than one passenger the boarding time is multiplied by the number of passengers. The load factor of each vehicle is assumed to be 1: during each turnaround all passengers de-board the aircraft and new passengers board the aircraft until all seats are occupied. The length of the passenger-related turnaround has corresponding duration.

Figure 3: *VoloCity* with two passengers and 11.3 m maximum distance (picture taken from 2021 white paper [24]).

Parameter	Value
Approach and landing time	99.2 s
Taxi speed	3.25 m/s
Taxi mode	Hover
Start/stop engines time	4.75 s
Passenger boarding time	92.7 s
Passenger de-boarding time	92.5 s
Take-off and departure time	72.2 s
Maximum dimension vehicle	11.3 m
Tip-to-tip span vehicle	11.3 m
Minimum distance FATO/FATO	200 ft (61 m)
Number of passengers	2
Turnaround time at gate	0 min // 20 min

Table 1: Input parameters required by vertiport sizing method including parameter value specification according to Preis et al. [33].

2.3 Definition of performance indicator

Scenarios will be measured and compared based on the performance indicator of "hourly passenger throughput per area" *T/h/A*. A vehicle throughput is defined as shown in figure 1. Accordingly an "hourly vehicle throughput of 1" means that one of the above described chain of operations (arrival, taxi to gate, turnaround including boarding, taxi to pad, departure) can take place within one hour on the given vertiport airfield. The hourly passenger throughput *T/h* is hourly vehicle throughput multiplied by the number of seats in the vehicle. Next, the hourly passenger throughput *T/h* is divided by the area of the vertiport airfield *A*. This yields the performance indicator "hourly passenger throughput per area" *T/h/A* as shown in equation 1. This indicator allows to directly compare vehicles and different sizes of vertiports and will be used throughout this paper.

$$T/h/A\left[\frac{PAX}{h*m^2}\right] = \frac{T_{max}}{t[h]} * \frac{1}{A_{airfield}[m^2]} \quad (1)$$

2.4 Evaluation baseline scenario

The cases *vertistop* and *vertihub* as defined in section 2.2 were simulated with the *VoloCity* as reference vehicle for areas from 100 - 10,000 m². The step size between areas is 100 m² and each area was considered in three variations as rectangles with aspect ratios 1:1, 1:2 and 1:3, yielding a total of 300 scenarios per case. In the following, three types of analysis will be presented, each dependent on the size of the vertiport airfield area: (1) the hourly passenger throughput, (2) the favored topology and (3) the optimal ratio of gates to pads. To create a linear fit all scenarios are considered, but for better readability only randomly selected datapoints are visualized in figure 4.

Here are a few initial observations: the vertistop achieves higher throughput than the vertihub, as can be expected, in particular for small areas. Yet, the slope of the linear fit is similar, which might allow the postulation that larger vertiports are able to cope with longer turnaround times without losing substantial throughput capacity. For the vertistop, the single topology is dominant for small areas and the linear topology becomes dominant for large areas. For the vertihub this transitions comes earlier. The satellite topology is also favored for various areas except very small and very large areas, while the pier topology is negligible. While the vertistop favors a gate to pad ratio of 3:1 for almost all areas, the optimal ratios for the vertihub range from two to seven gates per pad, with no obvious trend visible.

Expressing the results in a rule of thumb, the average value for *T/h/A* of all scenarios is calculated. For the vertistop the value is 0.015 PAX/h/m² and for the vertihub the value is 0.009 PAX/h/m². This means, on average, 0.015 and 0.009 passengers can be serviced per hour and square meter on a vertistop or a vertihub, respectively, when operating only *VoloCity* vehicles.

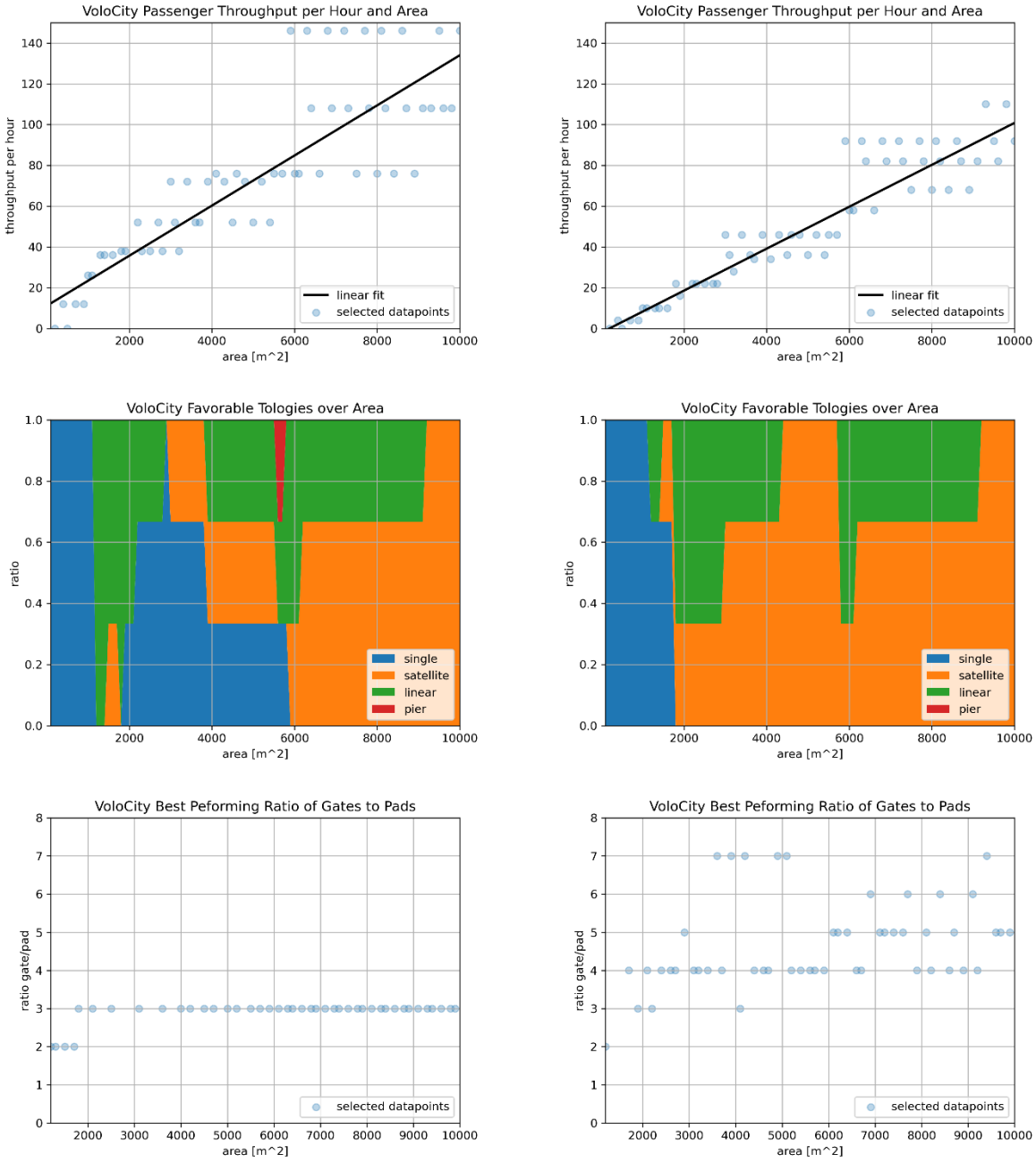

Figure 4: Evaluation of cases vertistop (left) and vertihub (right) over size of vertiport airfield.

3 Vehicle study

There are many ongoing eVTOLs development projects at this point, out of which some of the most well developed and promising vehicles will be compared according to their operational performance in this section. The performance indicator *T/h/A* will be used as explained in section 2.3. A total of 10 vehicles were chosen, which are either prominent in scientific literature or are close to receiving flight certification. For an extensive treatment of ongoing eVTOLs development projects please refer to [36–39].

3.1 Vehicle dimensions and passenger seats

eVTOLs come in many different configurations, out of which three are most prominent: multicopter, lift+cruise and the tilt-wing/prop configuration. Ten vehicles including their dimensions and number of seats are shown in table 2. The trend appears to be that for each extra seat the vehicle needs to be 1.17 m larger in its maximum dimensions plus a fixed dimension of 6.4 m (see figure 5). From this linear trend equation 2 was derived. Taking the seat to dimension ratio as a measure of operational performance, the *CityAirbus* and the *Lilium Jet* perform best and Airbus' *Vahana*, the previously considered *VoloCity* and *Kitty Hawk* (formerly Wisk), perform worst. For reasons of comparability between autonomous and (human) piloted configurations, the pilot seat was counted among the passenger seats. The maximum dimension of all vehicles is between 5-16 m; this range is chosen for further analysis.

Name	Tip-to-tip span [m]	Maximum dimension [m]	Total seats	Seats per maximum dimension [1/m]	Source
VoloCity	11.3	11.3	2	0.18	[35]
Vahana	5.7	6.25	1	0.16	[40]
Joby S4	10.7	10.7	4	0.37	[41]
eHang 216	5.61	5.61	2	0.36	[42]
Kitty Hawk	11	11	2	0.18	[43]
UBER	15.24	15.24	5	0.33	[44]
Aurora	9,14	9.14	2	0.22	[45]
ALIA-250	15.24	15.24	6	0.39	[46]
CityAirbus	8	8	5	0.63	[47]
Lilium Jet	8	13.9	7	0.50	[48]

Table 2: Operations-related performance data of prominent eVTOLs.

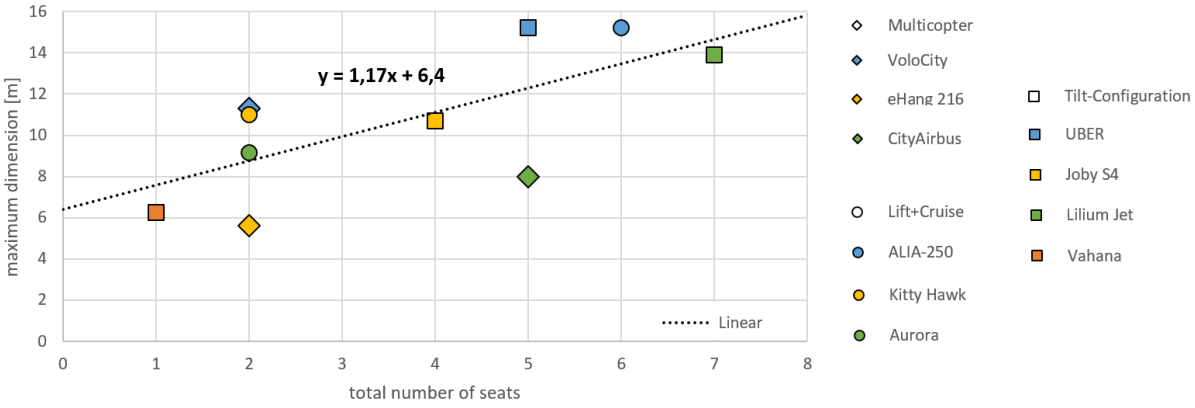

Figure 5: Relation seats to size of vehicle.

$$maximum\ dimension\ eVTOL = 1.17\ m * n_{Seats} + 6.4\ m \quad (2)$$

3.2 Dimensions of vertiport elements

Dimensions of pads, gates and taxiways are derived from the FAA "Heliport Design Guidelines" [32] (see figure 6) and their relationship to the maximum dimensions of the vehicle is visualized below (see figure 7). For pads the side length and area of the three squares (TLOF, FATO and Pad Safety) is displayed. For gates the diameter and area of the two circles (Gate Area and Gate Safety) is displayed with differentiated measures depending on the taxi-mode (hover or ground). For taxi-ways the breadth and area of a segment between two gates is displayed, also distinguishing between taxi-modes.

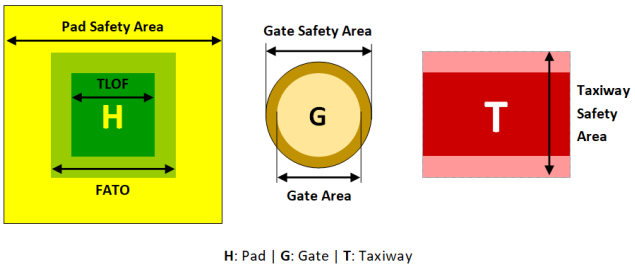

Figure 6: Dimensions of pads, gates and taxi-ways.

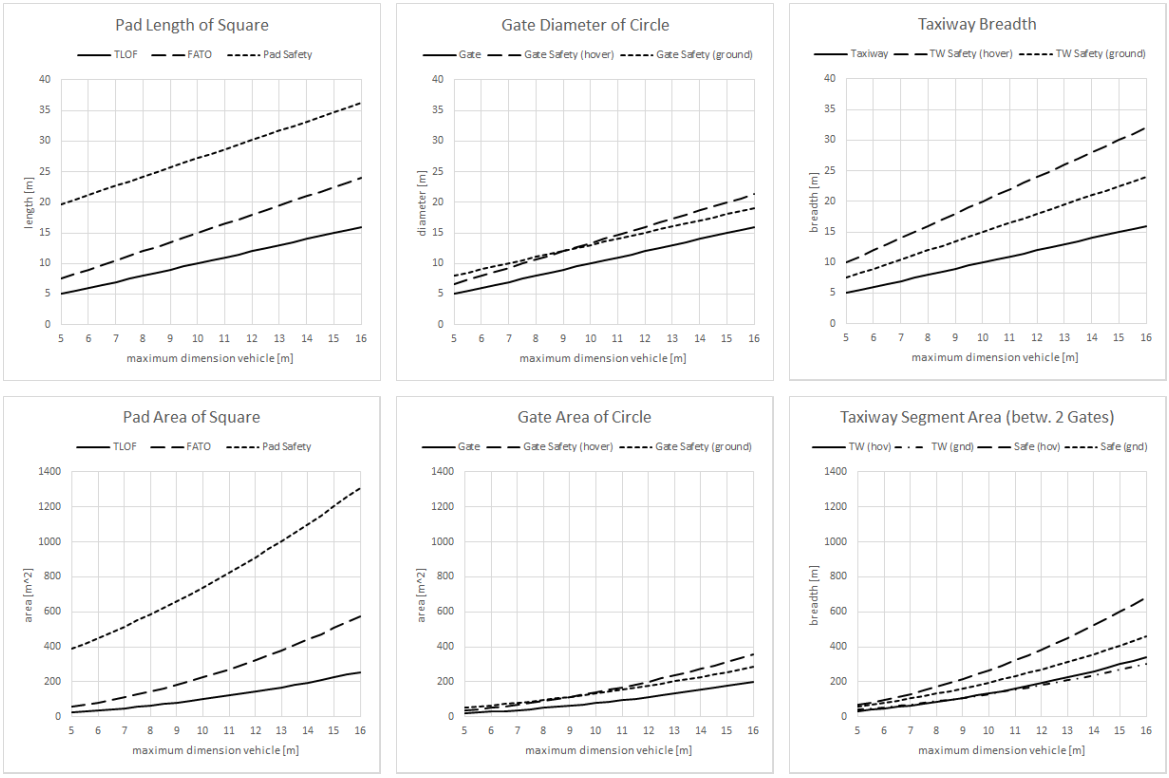

Figure 7: Visualization of length and area of vertiport elements.

Finding the best gate to pad ratio is an important factor in choosing the optimal vertiport layout, as was hinted on in section 2.4. The quotient of pad safety to gate safety is shown in figure 8. Different safety standards apply for gates (and taxi-ways) depending on the taxi-mode, which are treated in detail in the previous publication by Preis [26]. As can be seen in figure 8, there is a trade-off between the modes of taxi at around 9 m of maximum vehicle dimension. Generally speaking the slopes of both curves are falling, which can be interpreted as gates being more performant according to *T/h/A* for small vehicles compared to large vehicles, when being in the trade-off situation with pads. Or, in other words, small vehicle operators have an interest in freeing up pads quickly, because they are more "space-costly" in relative terms. The quotient shown in figure 8 is the number of gates that would fit into the same area as one pad.

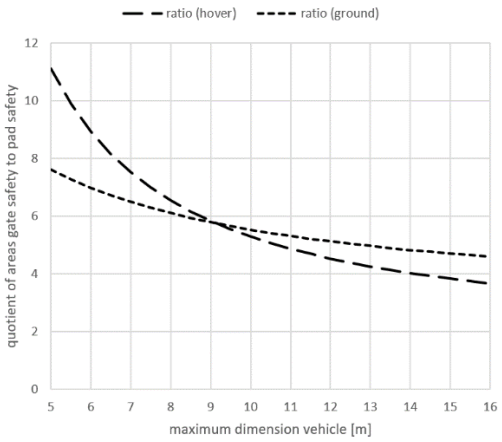

Figure 8: Comparing areas of pad safety and gate safety.

3.3 Prominent vehicle study results

The study from section 2.4 was executed analogous to the *vertistop* case for all ten vehicles listed in table 2 and compared according to their *T/h/A* (see section 2.3 for the definition of the performance indicator). The results are visualized in figure 9. The rules of thumb for *T/h/A* and the inverse equivalent of "area necessary to service one passenger throughput per hour" *A/T/h* can be found in table 3.

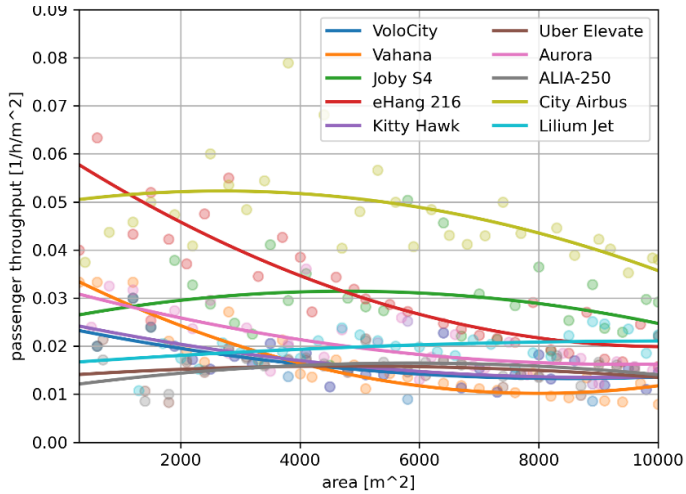

Figure 9: Relative vehicle throughput performance of different vehicles (quadratic fit).

Name	T/h/A [PAX/h/m²]	A/T/h [m²/PAX/h]
VoloCity	0.015	66.7
Vahana	0.014	72.2
Joby S4	0.029	34.7
eHang 216	0.029	34.2
Kitty Hawk	0.015	65.1
UBER	0.015	64.8
Aurora	0.019	53.8
ALIA-250	0.016	63.3
CityAirbus	0.045	22.1
Lilium Jet	0.020	51.3

Table 3: Operational vehicle performance according to hourly passenger throughput.

4 Safety margin study

Current vertiport design is often based on existing heliport design guidelines, while acknowledging the notion that regulations will most likely change in the future; this section explores the potentials of throughput gain by reducing established safety margins. Three aspects will be investigated: first, the size of safety areas around pads, gates and taxi-ways. Second, the minimum distance between the FATOs of two pads, which is necessary to operate the pads simultaneously. Third, the minimum separation between two aircraft during operations on the pads – this safety margin corresponds to the time a pad is occupied during an approach or departure sequence. The underlying assumption behind shrinking the safety margins is that the performance of eVTOLs will be superior to that of conventional helicopters due to electrification and automation. Therefore, existing safety margins might be unnecessarily high for future operations.

An indicator of "throughput improvement potential per safety margin reduction" will be defined at this point, to compare the various improvement potentials (see equation 3). As a base value the hourly passenger throughput per area *T/h/A* as defined in section 2.3 will be used. To define the improvement potential of the *T/h/A* the baseline case with full safety margins will be compared to a case *k* with reduced safety margins. The quotient of the two values is then divided by the relative reduction of safety margin, which yields the throughput improvement potential indicator ΔT. For example a $\Delta T = 0.5$ can be interpreted as follows: a 1% safety margin reduction yields a 0.5% increase in passenger throughput.

$$\Delta T = \frac{PAX/h/A_k}{PAX/h/A_{baseline}} * \frac{1}{\Delta\, Safety\ Margin} \tag{3}$$

4.1 Pad, gate and taxi-way safety areas

According to the FAA heliport design guidelines [32] pads, gates and taxi-ways need safety areas around their operational surface, which are either fixed, based on the vehicle dimensions or a mixture of both. The pad safety area

is larger than the FATO by the larger of 40 ft and 2/3 the maximum dimension of the vehicle. The size of the FATO in this analysis is not changed. The gate safety area is larger than the gate area by 1/3 of the maximum dimensions of the vehicle for hover taxiing or 10 ft for ground taxiing. The taxi-way safety area is larger than the breadth of the taxi-way by 1 tip-to-tip span for hover taxiing and 1/2 tip-to-tip span for ground taxiing. Analogue to the baseline scenario from section 2 hover taxiing is selected.

Five cases were defined in the following with 100%, 75%, 50%, 25% and 0% safety margin compared to the original safety margins for all three elements. The absolute and relative gains of *T/h/A* can be seen in figure 10. A general observation is that the throughput gains are larger for smaller vertiport layouts. The average throughput improvement potential while reducing all three safety areas simultaneously is $\Delta T_{mixed} = 0.63$. The increase in throughput for each case is shown in table 4.

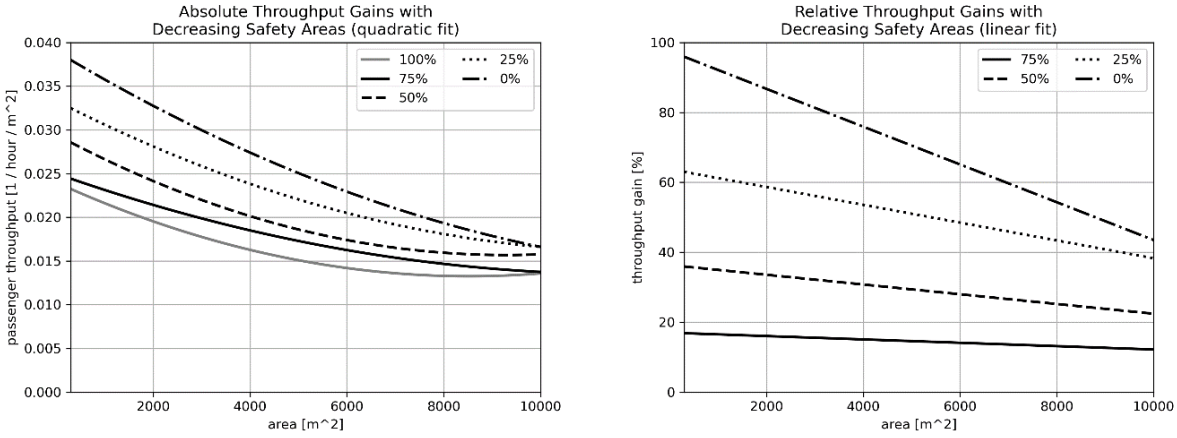

Figure 10: Absolute (left) and relative (right) throughput gain from decreasing safety margins.

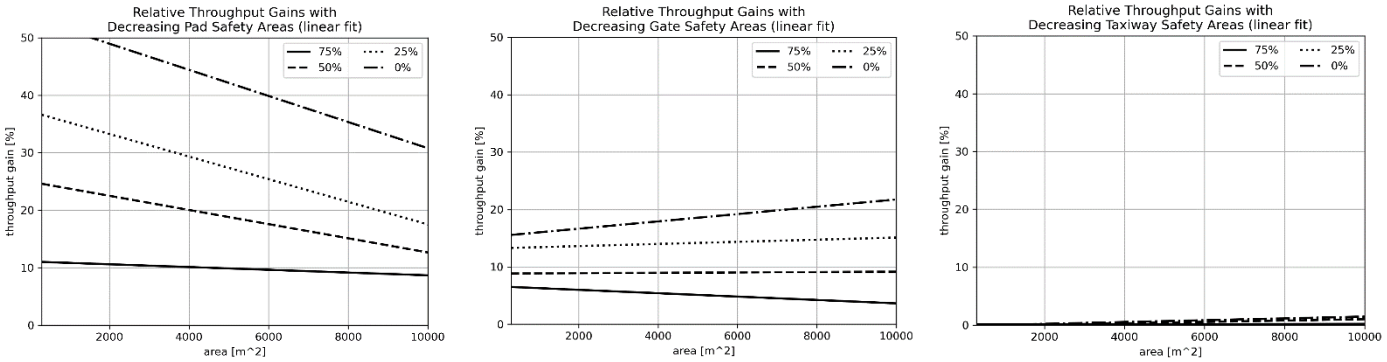

Figure 11: Relative throughput gains from decreasing safety margins for pads (left), gates (middle) and taxi-ways (right).

Case #	Safety margin size	Throughput gain mixed	Throughput gain pad	Throughput gain gate	Throughput gain taxi-way
1	100%	-	-	-	-
2	75%	14.4 %	9.8 %	5.0 %	0.1 %
3	50%	29.0 %	18.4 %	9.0 %	0.4 %
4	25%	50.3 %	26.8 %	14.2 %	0.6 %
5	0%	68.9 %	41.5 %	18.7 %	0.7 %
ΔT	**-**	**0.63**	**0.38**	**0.19**	**0.01**

Table 4: Overview of throughput gain from reducing vertiport element safety margin.

To identify the contribution to the throughput increase each element makes, pads, gates and taxi-ways are now investigated independently. The relative gains of *T/h/A* are presented in figure 11 and show that decreasing pad safety areas have a mayor impact (ΔT_{pad} = 0.38), gates safety areas a minor impact (ΔT_{gate} = 0.19) and taxi-way safety areas a negligible impact (ΔT_{taxi} = 0.01). Analogue to the mixed case above, the individual throughput increases for each case are laid out in table 4.

4.2 FATO/FATO minimum distance

The FAA heliport design guidelines recommend a 200 ft distance between the FATOs of two pads, in order to operate both pads simultaneously, which is desirable for vertiport operations. Analogue to the element study in section 4.1, five cases are considered with 100-0% minimum FATO/FATO distance compared to the baseline case. The absolute and relative gains of *T/h/A* can be seen in figure 12. Other than the element safety area study in section 4.1, in this case the throughput increase potential rises with larger vertiport areas. Further, it appears that small reductions in the minimum FATO/FATO distance yield little throughput increase, while large reductions cause over-proportionally strong throughput increase. The average throughput improvement potential is ΔT_{FATO} = 0.31. The increases in throughput for cases 2-5 are 1.9%, 11.4%, 36.8% and 44.3%, respectively.

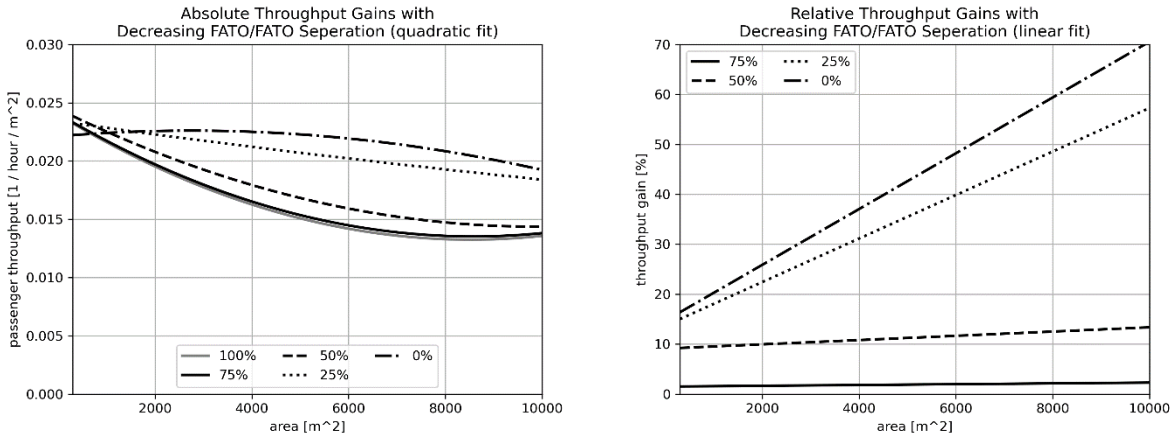

Figure 12: Absolute (left) and relative (right) throughput gain from decreasing FATO minimum distance.

4.3 Aircraft separation minima

Approach and departure times at vertiports are in part technical necessity to avoid vehicle collision and in part safety margin to ensure aircraft separation under imperfect, real-world operations. The latter part of the approach and departure process might be reduced with increasing vehicle performance, resulting in smaller time slots reserving a pad for an operation. In the following study aircraft separation of 90s down to 15s will be considered. The study parameters and results are listed in table 5 and absolute and relative gains of *T/h/A* are shown in figure 13. Similar to the FATO study, the largest throughput improvement potential lies with medium and larger vertiport areas. Further, the throughput improvement potential grows over-proportionally with the reduction in safety margin. The average throughput improvement potential is ΔT_{Sep} = 1.15.

Case #	Reduction aircraft separation minima [%]	Approach/departure time [s]	Throughput gain [%]
1	0	90	-
2	16.6	75	13.0
3	33.3	60	33.4
4	50	45	62.1
5	66.6	30	91.1
6	83.3	15	113.8

Table 5: Throughput gain from reducing aircraft separation minima.

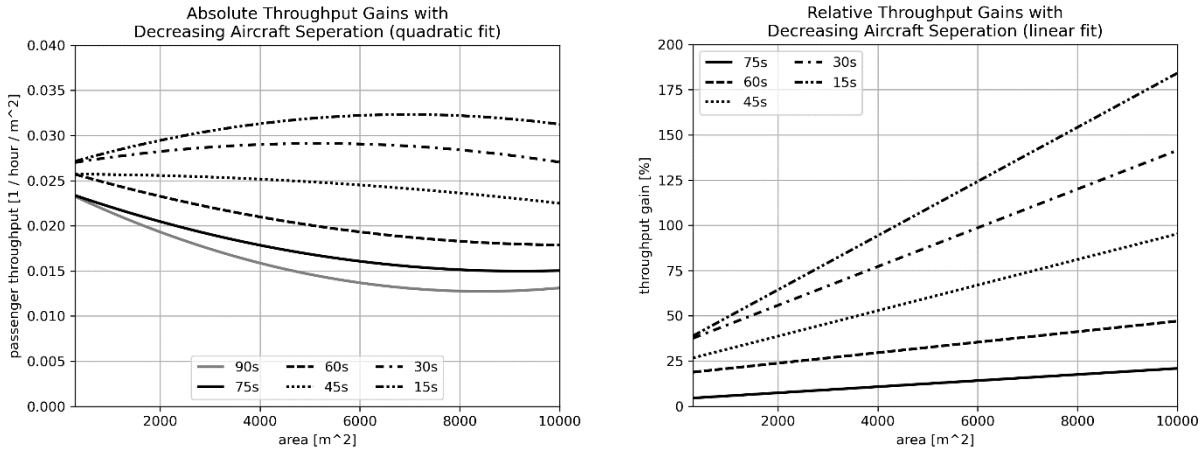

Figure 13: Absolute (left) and relative (right) throughput gain from decreasing aircraft separation minima.

5 Summary

Ground infrastructure is an essential part of the emerging transportation system of Urban Air Mobility, which has received only secondary attention so far. In particular the throughput capacities of vertiports is a research gap this paper attempts to address. An existing Mixed-Integer Programming approach [26] is applied to a range of vertiport scenarios to understand throughput capacities and sensitivities better. Vertiport airfield areas from 100-10,000 m² are considered with *VoloCity* as the reference design vehicle [35]. A baseline case is specified according to Preis et al. [33] and analyzed in two variations: as vertistop with no fixed turnaround time and as vertihub with 20 minutes turnaround time. The performance indicator "hourly passenger throughput per area" (*T/h/A*) is introduced, which results in values 0.015 and 0.009 for vertistop and vertihub, respectively.

In the next step, 10 prominent vehicles are investigated, finding that the approximated linear correlation between maximum vehicle dimension and the number of seats is as follows: the maximum dimension is 6.4 m plus 1.17 m for each seat on the aircraft. In the consecutive studies the *CityAirbus* performs best and *Vahana* performs worst; both vehicles designed by Airbus. All vehicles' *T/h/A* range from 0.014 to 0.045 PAX/h/m², which corresponds to 22-72 m² of vertiport airfield needed per hourly passenger throughput. Lastly, the "throughput improvement potential per safety margin reduction" (ΔT) is defined as a way of comparing vertiport sensitivities. The biggest potentials of increasing passenger throughput lie in reducing aircraft separation minima (ΔT_{Sep} = 1.15), pad safety area (ΔT_{pad} = 0.38), minimum FATO/FATO distance (ΔT_{FATO} = 0.31) and gate safety area (ΔT_{gate} = 0.19). The impact of reducing taxi-way safety area is negligible.

The established insights can help three groups of people in the broader context of UAM. First, other researchers in academia can benefit from applying the rules-of-thumb for passenger throughput as input in their studies, in particular for making realistic vertiport capacity constraint assumptions in UAM demand studies. Second, vehicle developers can use the presented analysis to understand the operational performance of their own vehicle both individually and in comparison with other vehicles. Beneficial operational environments are highlighted for different types of vehicles. Third, the FAA and other regulatory agencies can draw on the throughput improvement potentials presented in this paper when deciding how to formulate future versions of vertiport design guidelines.

References

[1] P. D. Vascik, "Systems Analysis Of Urban Air Mobility Operational Scaling," Ph.D., Department of Aeronautics & Astrophysics, Massachusetts Institute of Technology (MIT), Cambridge, Mass, 2020.

[2] R. Lineberger, A. Hussain, M. Metcalfe, and V. Rutgers, "Infrastructure barriers to the elevated future of mobility: Are cities ready with the infrastructure needed for urban air transportation?," Deloitte Insights, 2019.

[3] T. Johnston, R. Riedel, and S. Sahdev, “To take off, flying vehicles first need places to land: The buzz about vehicles flying above hides the infrastructure challenge below.,” 2020.
[4] P. D. Vascik and J. R. Hansman, “Scaling Constraints for Urban Air Mobility Operations: Air Traffic Control, Ground Infrastructure, and Noise,” in 18th AIAA ATIO Conference 2018, Atlanta, Georgia, USA, 2018.
[5] M. Giligan, J. D. Grizzle, and V. H. Cox, “Integration of Unmanned Aircraft Systems into the National Airspace System: Concept of Operations v2.0,” 2012.
[6] P. H. Kopardekar, “Unmanned Aerial System (UAS) Traffic Management (UTM): Enabling Low-Altitude Airspace and UAS Operations,” NASA Ames Research Center, Moffett Field, California, 2014.
[7] European Union Aviaton Safety Agency (EASA), Ed., “Concept of Operations for Drones: A risk based approach to regulation of unmanned aircraft,” 2015.
[8] K. Balakrishnan, J. Polastre, J. Mooberry, R. Golding, and P. Sachs, “Blueprint For The Sky: The roadmap for the safe integration of autonomous aircraft,” AIRBUS, 2018. [Online]. Available: https://www.airbusutm.com/
[9] G. Geister and B. Korn, “Concept for Urban Airspace Integration DLR U-Space Blueprint: Integrating UAS into the future aviation system,” Deutsches Zentrum für Luft- und Raumfahrt (DLR), 2017.
[10] Federal Aviation Administration (FAA), Ed., “Low Altitude Authorization and Notification Capability (LAANC) Concept of Operations,” 2017.
[11] Federal Aviation Administration (FAA) and U.S. Department of Transportation (DoT), Eds., “Urban Air Mobility (UAM): Concept of Operations v1.0,” 2020.
[12] D. P. Thipphavong et al., “Urban Air Mobility Airspace Integration Concepts and Considerations,” in 18th AIAA Aviation Technology, Integration, and Operations Conference 2018, Atlanta, Georgia, USA, 2018, p. 2018.
[13] European Union Aviaton Safety Agency (EASA), Ed., “U-SPACE REGULATORY FRAMEWORK WORKSHOP: SUMMARY OF CONCLUSIONS,” 2019.
[14] V. Sparrow et al., “Aviation Noise Impacts White Paper: State of the Science 2019: Aviation Noise Impacts,” 2019. [Online]. Available: https://www.icao.int/environmental-protection/Documents/Noise/
[15] P. D. Vascik and J. R. Hansman, “Evaluation Of Key Operational Constraints Affecting On-Demand Mobility For Aviation In The Los Angeles Basin: Ground Infrastructure, Air Traffic Control And Noise,” in 17th AIAA ATIO Conference, Denver, Colorado, USA, 2017.
[16] International Transport Forum and OECD, Eds., “Ready for Take-Off?: Integrating Drones into the Transport System,” 2021.
[17] K. A. Ackerman and I. M. Gregory, “Trajectory Generation for Noise-Constrained Autonomous Flight Operations,” in AIAA Scitech 2020 Forum, Orlando, FL, 2020.
[18] D. Phiesel and D. Moormann, “Bewertung des Bodenrisikos beim Betrieb von kleinen unbemannten Fluggeräten : Ein einfacher und quantitativer Ansatz,” in 66. Deutscher Luft- und Raumfahrtkongress, München, 2017.
[19] D. Duwe and A. Sprenger, “Acceptance, Preferences and Willingness to Pay Analysis for Flying Cars and Passenger Drones,” in 6th International Conference on Innovation in Science and Technology, London, 2019.
[20] R. Bonk et al., “Fit2Fly: A Proof of Concept for Testing the Commercial Feasibility of Unmanned Aerial System Operations,” in AIAA Scitech 2020 Forum, Orlando, FL, 2020.
[21] A. Straubinger, R. L. Rothfeld, M. Shamiyeh, K.-D. Büchter, J. Kaiser, and K. O. Plötner, “An overview of current research and developments in urban air mobility – Setting the scene for UAM introduction,” JATM, vol. 87, p. 101852, 2020, doi: 10.1016/j.jairtraman.2020.101852.
[22] L. A. Garrow, B. J. German, and C. E. Leonard, “Urban air mobility: A comprehensive review and comparative analysis with autonomous and electric ground transportation for informing future research,” Transportation Research Part C: Emerging Technologies, vol. 132, no. 2, p. 103377, 2021, doi: 10.1016/j.trc.2021.103377.
[23] A. Cohen, J. Guan, M. Beamer, R. Dittoe, and S. Mokhtarimousavi, “Reimagining the Future of Transportation with Personal Flight: Preparing and Planning for Urban Air Mobility,” 2020.
[24] Volocopter, Ed., “The Roadmap to scalable Urban Air Mobility: White Paper 2.0,” Bruchsal, Germany, 2021. Accessed: May 3 2021. [Online]. Available: https://www.volocopter.com/content/uploads/20210324_Volocopter_WhitePaper_Roadmap_to_scalable_UAM_m.pdf
[25] S. Rajendran and S. Srinivas, “Air taxi service for urban mobility: A critical review of recent developments, future challenges, and opportunities,” Transportation Research Part E: Logistics and Transportation Review, vol. 143, no. 2, p. 102090, 2020, doi: 10.1016/j.tre.2020.102090.

[26] L. Preis, “Quick Sizing, Throughput Estimating and Layout Planning for VTOL Aerodromes – A Methodology for Vertiport Design,” in AIAA Aviation 2021 Forum, virtual event, 2021. [Online]. Available: https://arc.aiaa.org/doi/10.2514/6.2021-2372

[27] P. D. Vascik and J. R. Hansman, “Development of Vertiport Capacity Envelopes and Analysis of Their Sensitivity to Topological and Operational Factors,” in AIAA Scitech 2019 Forum, San Diego, California, 2019.

[28] S. Zelinski, “Operational Analysis of Vertiport Surface Topology,” in 39th DASC - Digital Avionics Systems Conference: Virtual conference, October 11-16, conference proceedings, San Antonio, TX, USA, 2020.

[29] J. D. Petersen, R. J. Alexander, and S. S. Swaintek, “Dynamic Vertiport Configuration,” US 2020/0226937 A1, USA 16 / 248,170, Jun 16, 2020.

[30] International Organization for Standardization (ISO), ISO/AWI 5491: Vertiports — Infrastructure and equipment for Vertical Take-Off and Landing (VTOL) of electrically powered cargo Unmanned Aircraft System (UAS). [Online]. Available: https://www.iso.org/standard/81313.html (accessed: Jun. 1 2021).

[31] M. Hack Vazquez, “Vertiport Sizing and Layout Planning through Integer Programming in the Context of Urban Air Mobility,” master thesis, Technical University of Munich (TUM), Munich, 2021. [Online]. Available: https://mediatum.ub.tum.de/node?id=1624149

[32] Federal Aviation Administration (FAA), “Heliport Design,” AC No: 150/5390-2C, 2012. [Online]. Available: https://www.faa.gov/airports/resources/advisory_circulars/index.cfm/go/document.current/documentnumber/150_5390-2

[33] L. Preis and M. Hornung, “Vertiport Operations Modeling, Agent-Based Simulation and Parameter Value Specification” (submitted to MPDI Journal *Electronics*, Special Issue on “Urban Air Mobility”), 2022.

[34] L. Preis and S. Cheng, “Simulation of Individual Aircraft and Passenger Behaviour and Study of Impact on Vertiport Operations: (submitted to AIAA Aviation 2022),” in AIAA Aviation 2022 Forum, Chicago, IL, 2022.

[35] Volocopter, VoloCity: Design specifications, August 2019. Calculated approximations not yet tested in flight. [Online]. Available: https://www.volocopter.com/solutions/volocity/

[36] M. Shamiyeh, J. Bijewitz, and M. Hornung, “A Review of Recent Personal Air Vehicle Concepts,” in 6th CEAS Conference, 2017.

[37] Y. Liu, M. Kreimeier, E. Stumpf, Y. Zhou, and H. Liu, “Overview of recent endeavors on personal aerial vehicles: A focus on the US and Europe led research activities,” Progress in Aerospace Sciences, vol. 91, pp. 53–66, 2017, doi: 10.1016/j.paerosci.2017.03.001.

[38] R. Lineberger, A. Hussain, S. Mehra, and D. M. Pankratz, “Elevating the future of mobility: Passenger drones and flying cars,” Deloitte Insights, 2018.

[39] Y. Zhou, H. Zhao, and Y. Liu, “An evaluative review of the VTOL technologies for unmanned and manned aerial vehicles,” Computer Communications, vol. 149, no. 2, pp. 356–369, 2020, doi: 10.1016/j.comcom.2019.10.016.

[40] AIRBUS, Vahana: Our single-seat eVTOL demonstrator. [Online]. Available: https://www.airbus.com/en/innovation/zero-emission/urban-air-mobility/vahana (accessed: Dec. 21 2021).

[41] Joby Aviation, Joby S4. [Online]. Available: https://www.jobyaviation.com/ (accessed: Dec. 21 2021).

[42] eHang, EHang AAV: The Era of Urban Air Mobility is Coming. [Online]. Available: https://www.ehang.com/ehangaav (accessed: Dec. 21 2021).

[43] Kitty Hawk, Everyday flight for everyone. [Online]. Available: https://www.kittyhawk.aero/ (accessed: Dec. 21 2021).

[44] UBER Elevate, “UberAir Vehicle Requirements and Missions,” 2018. Accessed: Oct. 5 2021. [Online]. Available: https://s3.amazonaws.com/uber-static/elevate/Summary+Mission+and+Requirements.pdf

[45] Aurora Flight Sciences, Urban Air Mobility: Passenger Air Vehicle (PAV). [Online]. Available: https://www.aurora.aero/urban-air-mobility/ (accessed: Dec. 22 2021).

[46] BETA Technologies, Aircraft ALIA-250. [Online]. Available: https://www.beta.team/aircraft/ (accessed: Feb. 11 2022).

[47] AIRBUS, Airbus CityAirbus. [Online]. Available: https://transportup.com/airbus-cityairbus/ (accessed: Dec. 22 2021).

[48] P. Nathen, A. Bardenhagen, A. Strohmayer, R. Miller, S. Grimshaw, and J. Taylor, “Architectural performance assessment of an electric vertical take-o and landing (e-VTOL) aircraft based on a ducted vectored thrust concept,” 2021. Accessed: Dec. 21 2021. [Online]. Available: https://lilium.com/files/redaktion/refresh_feb2021/investors/Lilium_7-Seater_Paper.pdf